PAPER

Check for updates

Investigation of the radical scavenging potential of vanillin-based pyrido-dipyrimidines: experimental and *in silico* approach

Nenad Janković, [iD] *[a] Julijana Tadić,[b] Emilija Milović,[a] Zoran Marković, [iD] [ac] Svetlana Jeremić, [iD] [c] Jelena Petronijević,[d] Nenad Joksimović, [iD] [d] Teona Teodora Borović[e] and Syed Nasir Abbas Bukhari[f]

Antioxidants have a significant contribution in the cell protection against free radicals which may induce oxidative stress, and permanently damage the cells causing different disorders such as tumors, degenerative diseases, and accelerated aging. Nowadays, a multi-functionalized heterocyclic framework plays an important role in drug development, and it is of great importance in organic synthesis and medicinal chemistry. Encouraged by the bioactivity of the pyrido-dipyrimidine scaffold and vanillin core, herein, we made an effort to thoroughly investigate the antioxidant potential of the vanillin-based pyrido-dipyrimidines A–E to reveal novel promising free radical inhibitors. The structural analysis and the antioxidant action of the investigated molecules were performed *in silico* by DFT calculations. Studied compounds were screened for their antioxidant capacity using *in vitro* ABTS and DPPH assays. All the investigated compounds showed remarkable antioxidant activity, especially derivative A exhibiting inhibition of free radicals at the IC_{50} value (ABTS and DPPH assay 0.1 mg ml^{-1} and 0.081 mg ml^{-1}, respectively). Compound A has higher TEAC values implying its stronger antioxidant activity compared to a trolox standard. The applied calculation method and *in vitro* tests confirmed that compound A has a strong potential against free radicals and may be a novel candidate for application in antioxidant therapy.

Introduction

Antioxidants have gained attention in numerous research fields comprising medicinal chemistry, biomedicine, and clinical trials, mainly due to their therapeutic properties and beneficial effects on human health and wellbeing.[1] Oxidative stress – an imbalance of free radicals (RONS – reactive oxygen and nitrogen species) and antioxidants in cells – causes damage to biomolecules (DNA, protein, lipids) resulting in pathophysiological changes of cells.[2] These changes can be associated with certain conditions such as allergic diseases,[3] cancer,[4] cardiovascular,[5] immune,[6] and age-related diseases including neurodegenerative disorders such as Alzheimer's disease (AD)[7] and Parkinson's

disease (PD).[8] However, molecules with antioxidant activity inhibit free radical reactions and delay or prevent cellular damage.[9] Recent studies have suggested that antioxidant-based treatments can reduce the effect of RONSs and counteract oxidative stress providing promising therapy for patients suffering from cancer, AD, PD, and other degenerative conditions, and subsequently promoting healthy longevity.[10] Therefore, development of redox medicine and application of antioxidants are an emergency need.[11–14]

Among the N-containing heterocycles, pyrimidine derivatives are in particularly important building blocks in pharmaceuticals' design exhibiting a remarkable therapeutic potential.[15] Moreover, when pyrimidine moiety is fused with other heterocycles it results in the compounds with even more powerful activity. Such the compounds are the pyrido[2,3-*d*] pyrimidines which have broad spectrum of medicinal applications.[16] Namely, pyridopyrimidine molecule is a notable pharmacophore in drug design due to its various pharmacological actions including anticancer,[17] antioxidant,[18] analgesic,[19] anti-inflammatory,[20] and antimicrobial activity.[21] Furthermore, some pyridopyrimidine derivatives have been under the clinical trials for treatment of different cancers, and 22 of them are being used in the clinic for cancer treatment (FDA approval).[22,23]

On the other hand, vanillin is a natural compound, produced from the renewable sources on industrial level, and presenting

[a]University of Kragujevac, Institute for Information Technologies, Department of Sciences, Jovana Cvijića bb, 34000 Kragujevac, Serbia. E-mail: nenad.jankovic@uni.kg.ac.rs

[b]Vinča Institute of Nuclear Sciences – National Institute of the Republic of Serbia, University of Belgrade, Mike Petrovića Alasa 12-14, 11351 Vinča, Belgrade, Serbia

[c]The State University of Novi Pazar, 36300 Novi Pazar, Serbia

[d]University of Kragujevac, Faculty of Science, Department of Chemistry, Radoja Domanovića 12, Kragujevac, Serbia

[e]Faculty of Sciences, University of Novi Sad, Trg Dositeja Obradovića 3, 21000 Novi Sad, Serbia

[f]Department of Pharmaceutical Chemistry, College of Pharmacy, Jouf University, Sakaka, Al Jouf, 72388, Saudi Arabia

a significant tool in the synthesis of fine chemicals.[24] This phenolic molecule possesses strong biological potential and highlighted antioxidant properties.[25] Furthermore, vanillin derivatives are reported to be promising multi-target drugs for the treatment of degenerative diseases having adequate pharmacokinetic and pharmacodynamic characteristics.[25]

In the light of the studies, and in the extension of our recently published work[24] on the design of bioactive vanillin-based pyrido-dipyrimidines, in presented study, we thoroughly investigated the antioxidant capability of the synthetized molecular hybrids using *in silico* (DFT) and *in vitro* approaches (ABTS and DPPH assays), in order to discover much needed new candidates for treatment of different redox-related conditions.

Results and discussion

The antioxidant activity of selected compounds (Fig. 1) was further evaluated by determination of the IC_{50} values. IC_{50} represent the concentration of sample able to scavenge 50% of ABTS or DPPH radicals in the solution, and high IC_{50} values generally suggest low antioxidant activity. The solutions of pyrido-dipyrimidine in methanol/PBS solution, as well as solutions of ABTS or DPPH were prepared and obtained IC_{50} were compared (Table 1). The tests were performed in triplicate.

Compounds **A–E** have been evaluated for their IC_{50} and TEAC (Trolox Equivalent Antioxidant Capacity) values. Solutions of **A–D**, in concentration range from 0.0125–1 mg ml^{-1}, were prepared and IC_{50} values were established, and consequently, the TEAC values were calculated (Table 1). The

antioxidant activity based on IC_{50} and TEAC values of tested compounds is presented in Table 1. All investigated compounds exhibited remarkable antioxidant potential. Namely, analysed compounds exhibited excellent antioxidant activity (the inhibition was up to 99%), three molecules expressed good ability to scavenge the ABTS$^{•+}$ radical cation while all tested compounds showed very good antioxidant properties in comparison with DPPH radical (Table 1). Considering the results presented in Table 1 it can be determined that investigated compounds not just exhibited remarkable capacity to inhibit ABTS$^{•+}$ or DPPH radical, but also molecules **A–D** showed higher TEAC than Trolox standard indicating a strong potential against free radicals. In comparison to Trolox, compounds **A–D** exhibited high inhibition of DPPH radicals up to 96% confirming strong antioxidant potential. TEAC values for DPPH were in range 2.88 to 1.17. Molecules **A** and **B** showed the best TEAC values for ABTS. The presence additional hydroxy group at *m*-position could be crucial for such a high activity of molecule **A** in both assays.

Taking into account presented results, it can be seen that investigated compounds displayed powerful antioxidant activity indicating their promising potential for application as novel antioxidants.

In addition, compounds **A–E** were exposed to cytotoxic activity against normal fibroblast MRC-5. Delivered IC_{50} values for all investigated compounds (IC_{50} >200 μM) were showed significant non-toxic effect to MRC-5 cell lines.

In order to explore antioxidative mechanism at molecular level for two most active compounds (**A** and **B**) further investigation was performed by using computational approach. Conformational analyse, performed to find the most stable conformation of the estimated compounds, give the appropriate torsion angles values.

Values of the $\tau1$, $\tau2$, $\tau3$, $\tau4$ and $\tau5$ dihedral angles that correspond to the energy minima for molecule **A** are 8.73°, 3.59°, 81.34°, 100.08° and 0.16° respectively, and for molecule **B** they are 0.02°, 0.01°, 60.85°, 88.68° and 0.07° respectively (Fig. 2). The calculated angle values indicate significant deviation from the planarity of both investigated molecules.

Antioxidant activity of some molecule can be manifested by the easiness of releasing the hydrogen atom, and the formation of a more stable radical than the starting. The values of thermodynamic parameters can be used to determine which of the investigated reaction mechanisms is the most likely reaction
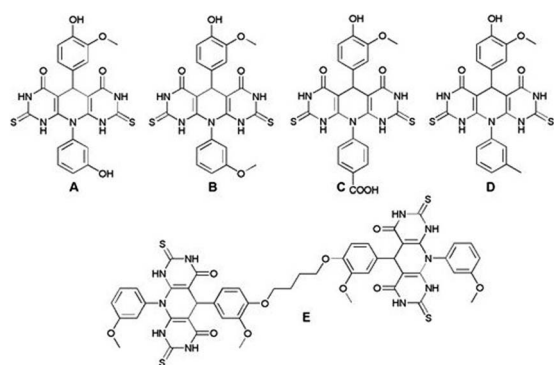

Fig. 1 Structures of investigated pyrido-dipyrimidines A–E.

Table 1 The IC_{50} values (mg ml^{-1}) of selected pyrido-dipyrimidines

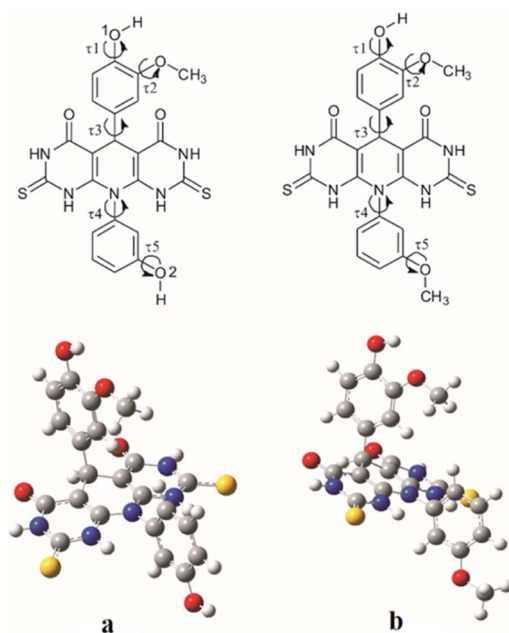|	ABTS			DPPH		
	I (%)	IC_{50}	TEAC	I (%)	IC_{50}	TEAC
A	99.9 ± 0.01	0.100 ± 0.003	2.54 ± 0.09	95.92 ± 0.14	0.081 ± 0.005	2.884 ± 0.161
B	99.99 ± 0.01	0.200 ± 0.006	1.27 ± 0.04	93.15 ± 0.13	0.199 ± 0.013	1.174 ± 0.066
C	99.12 ± 0.13	0.370 ± 0.013	0.69 ± 0.02	92.26 ± 0.13	0.144 ± 0.009	1.622 ± 0.090
D	99.99 ± 0.01	0.240 ± 0.008	1.06 ± 0.04	96.20 ± 0.15	0.124 ± 0.008	1.884 ± 0.106
E	99.99 ± 0.01	0.390 ± 0.013	0.65 ± 0.02	94.22 ± 0.18	0.195 ± 0.013	1.198 ± 0.067
Trolox	93.16 ± 0.12	0.250 ± 0.009	1 ± 0	96.17 ± 0.17	0.234 ± 0.015	1 ± 0

Fig. 2 Investigated torsion angles (τ1, τ2, τ3, τ4 and τ5) for molecules **A** (a) and **B** (b) (upper) and their optimized geometries (down).

Table 2 Reaction enthalpies (in kJ mol^{-1}) for the antioxidant radicals' formation for **A** and **B** calculated in water, methanol and benzene

		HAT	SPLET		SET-PT	
		BDE	PA	ETE	IP	PDE
Water	**A**–O1	350	178	349	506	21
	A–O2	466	140	503	506	137
	B	352	181	350	509	21
Methanol	**A**–O1	350	173	361	525	9
	A–O2	466	133	517	525	125
	B	353	175	362	528	9
Benzene	**A**–O1	359	452	330	634	148
	A–O2	465	369	520	634	254
	B	359	455	327	634	149

path for free radical scavenging. Table 2 shows the values of these parameters for the molecules **A** and **B** computed in water, methanol and benzene as the solvents.

Radicals and anions of the A and B molecules

The homolytic breaking of the O–H bonds in **A** and **B** results in formation of the corresponding radicals (Fig. 4). The stability of the formed radicals in methanol plays the main role in determining the antioxidant activity of the investigated molecules. The obtained values of BDE are given in Table 2, and the lower the BDE, the more stable the radical. Molecule **A** can form two radicals since it can undergo to the homolytic cleavage of the two O–H groups. According to the BDE values from Table 2, the radical formed in position 1 (**A**–O1 radical) is more stable than the radical in position 2 (**A**–O2 radical). Comparing spin density distributions of **A**–O1 and **A**–O2 radicals (Fig. 3), it can be
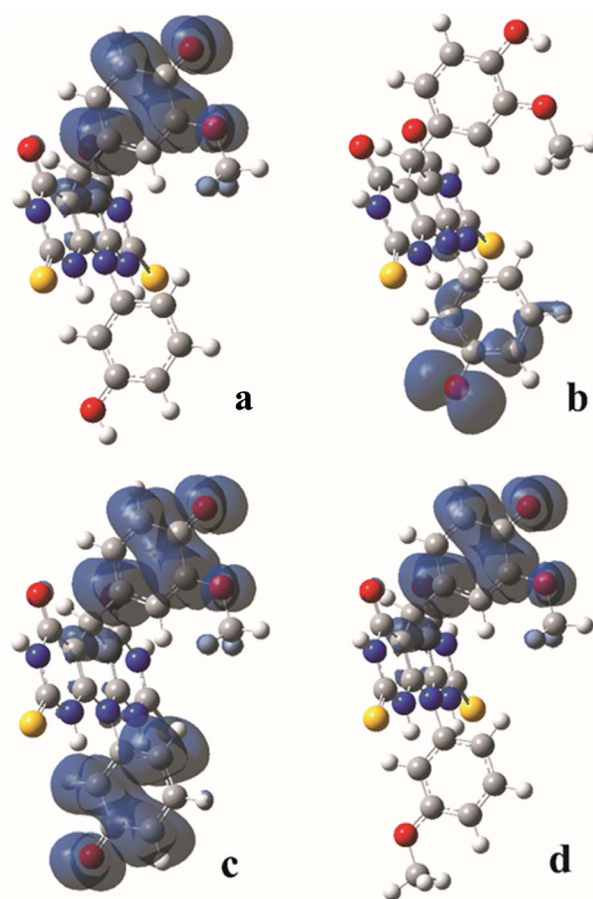

Fig. 3 Spin density distribution (only positive isovalues) in the corresponding radical species of the **A** and **B** molecules calculated in methanol: **A**–O1 radical (a); **A**–O2 radical (b); **A** diradical (c); **B** radical (d).

concluded that the unpaired electron in radical **A**–O1 is delocalized not only over the atoms of the corresponding benzene ring, but also through some atoms of the central tricyclic part of the molecule. On the other hand, the delocalization of the unpaired electron of radical **A**–O2 involves only the atoms of the corresponding benzene ring. The spin density distribution of **B** is similar to the spin density distribution of **A**–O1, which is in accordance with the similar values of their BDEs.

It must be mentioned that molecule **A** can homolytic release hydrogen atoms at both active positions simultaneously. This leads to the formation of a diradical species. Having on mind that **A**–O1 is more stable, the higher tendency to undergo to the further stabilisation due to diradical formation possess **A**–O2 radical.[26,27] The enthalpies of the diradical formation following homolytic breaking of the remaining O–H bond starting from the **A**–O2 are: 270 kJ mol^{-1}, 271 kJ mol^{-1} and 285 kJ mol^{-1} in water, methanol and benzene respectively. When the diradical is formed starting from the **A**–O1 radical, the values of the corresponding enthalpies are: 386 kJ mol^{-1}, 386 kJ mol^{-1}, and 391 kJ mol^{-1} in water, methanol and benzene respectively. The delocalization of unpaired electrons in this diradical forms include both benzenoid parts of the molecule (Fig. 4). The spin density distribution excludes the central tricyclic part of the
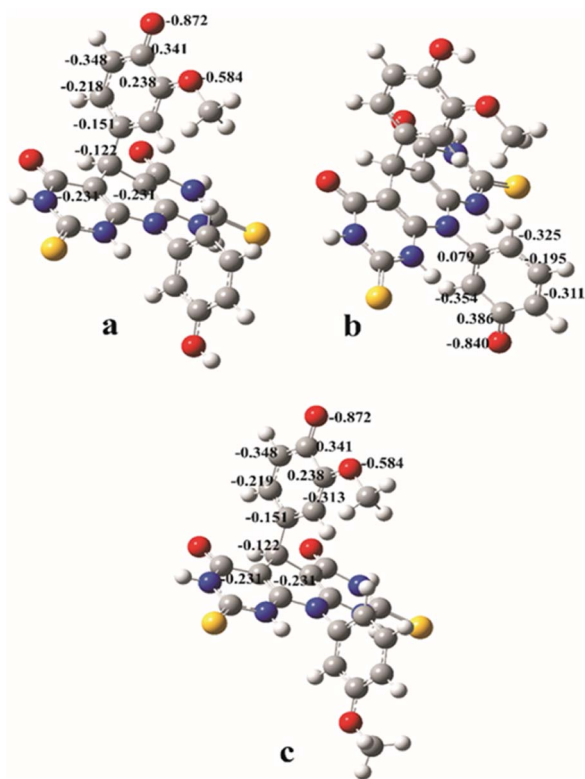
Fig. 4 The natural charge distributions in the most stable anions formed from the A and B molecules calculated in methanol: anion A–O1 (a); anion A–O2 (b); anion B (c).

molecule, which is a consequence of the non-planarity of the system.

Therefore, the higher antioxidant capacity of molecule A can be explained by the easiness of formation of triplet diradicals from monoradical species.[26,27] In addition, the fact is that on this molecule antioxidant processes can take place in two positions simultaneously. This is in agreement with the previously established fact that the antioxidant capacity of the compound increases with the increase in the number of hydroxyl groups.[28,29] The molecule B can achieve its antioxidant activity only through one active position, forming monoradical moiety.

The most plausible mechanism for the stable antioxidant radical formation can be discussed based on the BDE, PA and IP values. These values correspond to the enthalpy of the first reaction step of the appropriate mechanisms. The lowest enthalpy value corresponds to the most plausible mechanistic pathway. In order to be able to discuss the different behaviour of antioxidants depending on the polarity of the environment, the corresponding thermodynamic parameters were calculated in water ($\varepsilon = 78.36$), methanol ($\varepsilon = 32.61$) and benzene ($\varepsilon = 2.27$). Water was chosen as a typical polar medium, and also as the dominant solvent in which the DPPH analysis was performed. Methanol is a polar solvent, the molecules of which are small in size. Therefore, its solvation effect, which is a consequence of the formation of intermolecular hydrogen bonds with the dissolved molecule, is similar to that of water.[30,31] In

addition, the ABTS test was performed in this solvent, so for the sake of comparability of theoretical and experimental results, part of the calculation was performed in methanol. Benzene was chosen as a typical non-polar solvent, in order to simulate the behaviour of antioxidants in a lipid environment. It was observed that the values of thermodynamic parameters calculated in benzene corresponded most closely to the experimentally obtained results that indicate the antioxidative activities in a lipid environment.[32]

Since PA values are significantly lower than BDEs and IPs, one can conclude that SPLET is the most favourable reaction mechanism for both estimated molecules in polar solvents. The product of the first step of the SPLET is an anionic species. The resulting anions can be surrounded by water or methanol molecules, and thus stabilized by the solvation effect. Because of this, in polar solvents, SPLET appears as the dominant reaction mechanism. The lowest PA value corresponds to the anion of A molecule, indicating its higher antioxidant capacity. This is in accordance with the experimentally obtained results. A has two hydroxyl groups and thus two potential positions for antioxidant reactions. The PA value that corresponds to the cleavage of the O–H bond in position 2 is lower (A–O2 anion), and it indicates that it is more reactive position for antioxidative action over SPLET than the O–H bond in position 1 (A–O1 anion). The explanation of this phenomenon lies in the natural charge distribution of the appropriate anionic species (Fig. 4). The value of the natural charge at the O1 atom of the anion A–O1 is lower (-0.872) and more localised than negative charge at the atom O2 of the anion A–O2 (-0.840), calculated in methanol. It indicates better natural charge distribution at anion A–O2 over the neighbour atoms, and at the same time, its higher stability. It can be noticed that the values of the natural charges of anions A–O1 and B are almost equal. This indicates almost equal stability of these two anions, and it agrees with the similarities of the corresponding PA values from Table 2.

Since IP values are very high, the SET-PT mechanism is the lowest plausible mechanistic pathway in considering conditions. This can be explained by the fact that in the first step of SET-PT radical-cation is formed. When the reaction leads to the formation of the relative stable product, the appropriate thermodynamical parameters are low. On the other hand, the formation of unstable species is characterized by high values of thermodynamic parameters. Bearing that in mind, one can conclude that the radical-cation, created in the first step of the
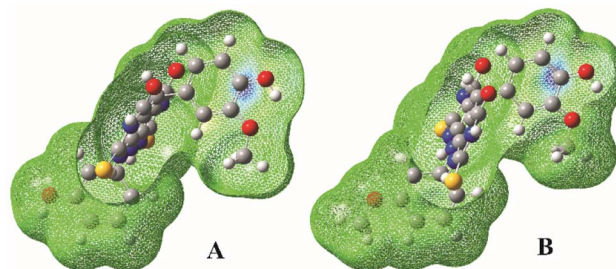

Fig. 5 Total spin density distribution in the radical cations of the A (left) and B (right) molecules calculated in methanol.

SET-PT is unstable specie. It is also known that the radical-cation is a highly reactive species, with high oxidation potentials,[29,30] so this explains the difficulty of its formation.[33,34] The instability and high reactivity of here formed radical-cations can be explained by the high localisation of the positive charge at the carbon atom linked to the hydroxyl-group of interest for radical reaction (Fig. 5).

Conclusions

Theoretical investigations included two molecules with the highest experimentally determined antioxidative capacity. Molecule **A** has two, and molecule **B** has one active position for antioxidative reaction. Both molecules show a tendency to follow a SPLET mechanism as the dominant mechanism of antioxidant action in polar environment, while in non-polar conditions predominant mechanism is HAT. In the first step of SPLET, the corresponding anion is formed. This anion can be stabilized in methanol and water as the solvents by the solvation effect. The greater stability of the **A**–O2 anion than that of anion of **B** is in agreement with the experimentally determined the highest antioxidant capacity of **A** molecule and is the consequence of the better natural charge distribution at anion **A**–O2 over the neighbours atoms. By comparing BDE values and spin density distributions, conclusions can be brought about the stability of antioxidant radicals, and the easiness of their formation by homolytic breaking of the O–H bond. It was found that the BDEs and spin density distributions for the mono-radical forms of both molecules are similar. On the other hand, the BDE value corresponding to the formation of diradical of molecule **A** is significantly lower than all BDEs for the formation of monoradicals. Also, the distribution of unpaired electrons of the resulting diradical covers the largest surface area of the molecule. Taking it on mind one can conclude that molecule **A** achieves its antioxidant activity through both active positions simultaneously, forming a diradical. Moreover, here obtained theoretical results are in accordance with the experimental ones.

Experimental section

Antioxidant activity

ABTS assay. The antioxidant activity of investigated compounds was determined by the ABTS radical-scavenging assay.[35] A stock solution of the ABTS radical cation was prepared in the reaction of ABTS (4.912 ml, 7 mM in phosphate-buffered saline (PBS)) and potassium persulfate (0.088 ml, 140 mM in distilled water). After 16 h of incubation in the dark, the stock solution was diluted with PBS until absorbance recorded at 734 nm was 0.700 ± 0.020. Subsequently, 20 μL of the compound solutions (1 mg of corresponding compound in 1 ml of PBS) were mixed with 2 ml of the ABTS solution, shaken and stored in the dark for 6 min. Afterwards the absorbance was measured at 734 nm. Each test was done in triplicate and the results were expressed as means $\pm$ SD. The inhibition percentage of ABTS radical cation was calculated using the formula:

$$\text{Inhibition } (\%) = (A_c - A_s)/A_c \times 100$$

where A_c is the absorbance of the control solution (20 μL of PBS in 2 ml of ABTS solution) and A_s is the absorbance of the sample solution. The antioxidant activity of most potent compounds was further evaluated by determination of the IC_{50} values and TEAC (Trolox Equivalent Antioxidant Capacity). The solutions of selected compounds and Trolox solution in PBS, were prepared at the concentrations of 1, 0.5, 0.25, 0.125 and 0.0125 mg ml^{-1}, and TEAC was calculated using following formula:[36]

$$\text{TEAC} = IC_{50} \text{ (Trolox)}/IC_{50} \text{ (tested compound)}$$

DPPH assay. In addition to ABTS assay, DPPH test was performed to study antioxidant activity of most potent compounds. The assay was done as described by Kundu *et al.*[36] Briefly, the DPPH solution was freshly prepared by dissolving DPPH in methanol (concentration of DPPH solution at 0.1 mM) and homogenizing in an ultrasonic bath for 30 s. Then, the solutions of the compounds, and the solution of Trolox as standard, were prepared at concentrations 1, 0.5, 0.25 and 0.125 and 0.0125 mg ml^{-1}. Sample solutions (100 μl) was mixed vigorously with 900 μl of the DPPH solution, and the mixture was incubated in the dark at room temperature for 30 min. Then, the absorbance of the solution was measured at 517 nm. Each test was done in triplicate and the results were expressed as means $\pm$ SD. The inhibition percentage of DPPH was calculated using the formula:

$$\text{Inhibition } (\%) = [1 - (A_s - A_b)/A_c] \times 100$$

where A_c is the absorbance of the control solution (100 μl of methanol in 900 μl of the DPPH solution) and A_s is the absorbance of the sample in DPPH solution, and A_b is absorbance of the sample in methanol.

TEAC values were calculated as described above.

DFT study

The DFT method was utilized to gain a better knowledge of the antioxidant capability of the studied compounds. According to the experimental findings, the compounds **A** and **B** were shown to be more potent antioxidants than the other evaluated substances. As a result, these two compounds were used for *in silico* investigations. The conformational analysis of the **A** and **B** molecules was done. For this purpose, different conformations were obtained by the rotations around the single bonds of interest. Each torsion angle was scanned in steps of 10° with no constraints on any other geometrical parameters. The geometry corresponding to the energy minimum for each analysed torsion angle was then used to optimize the geometry with the minimal energy values for investigated molecules, as well as to calculate the appropriate thermodynamically parameters. The geometry optimizations and frequency calculations of investigated molecules were performed using DFT/M06-2X functional[37] in conjunction with the 6-311++G(d,p) basis set,[38] implemented in the Gaussian 09 program package.[39] This

functional gives satisfactory results in the thermochemical and kinetic calculations and has been used widely by numerous authors.[40–42] The restricted calculations are used for moieties with paired electrons, while the unrestricted calculations are performed for moieties with unpaired electrons. Therefore unrestricted calculations applied for radicals and diradicals in a doublet and a triplet state can give us reliable and comparable values. To obtain the results comparable with the experimentally ones, all calculations were carried out in water, methanol and benzene, using the CPCM solvation model.[43] Spin density distribution and natural charge distribution in radical and ionic species were determined in methanol ($\varepsilon = 32.61$) as a solvent with an average value of the dielectric constant among the three solvents used here. To determine distribution of natural charge in ionic moieties, as well as to determine the spin density distribution in radical forms, NBO analysis is performed.[44,45] Potential energy minima for all the optimized species are verified by the absence of the imaginary frequencies. All calculations were done at 298.15 K.

The scavenging of free radicals appears to play an essential role in phenolic compounds' antioxidant action. The capacity of phenolic compounds to transfer their phenolic H-atom to a free radical is associated with their antiradical abilities. Several mechanistic pathways can be used to describe this process. Among the most investigated are HAT (Hydrogen Atom Transfer), SPLET (Sequential Proton Loss Electron Transfer) and SET-PT (Single-Electron Transfer followed by Proton Transfer).[46–49] The process describing the homolytic breakage of the O–H bond is known as HAT (eqn (1)). The capabilities of this mechanism are estimated based on BDE (Bond Dissociation Enthalpy) values (eqn (1a)).
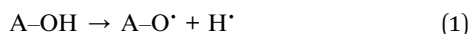
$$A\text{–}OH \rightarrow A\text{–}O^{\bullet} + H^{\bullet} \qquad (1)$$

$$BDE = H(A\text{–}O^{\bullet}) + H(H^{\bullet}) - H(A\text{–}OH) \qquad (1a)$$

In the previous equations A–OH, A–O$^{\bullet}$ and H$^{\bullet}$ denote antioxidant molecule, antioxidant radical and hydrogen atom, while $H(A\text{–}OH)$, $H(A\text{–}O^{\bullet})$ and $H(H^{\bullet})$ present their enthalpies respectively.

The SPLET mechanism is a two-step process. Dissociation happens in the first stage of the reaction, resulting in the formation of a proton (H$^+$) and an antioxidant anion (A–O$^-$). The second phase involves electron transfer (e$^-$), which is followed by the formation of the appropriate radical (eqn (2)). The PA value (Proton Affinity, eqn (2a)) may be used to describe the first step of the reaction, and the ETE value can be used to describe the second step (Electron Transfer Enthalpy, eqn (2b)).

$$A - OH \xrightarrow{-H^+} A - O^- \xrightarrow{-e^-} A - O^{\bullet} \qquad (2)$$
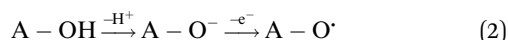
$$PA = H(A\text{–}O^-) + H(H^+) - H(A\text{–}OH) \qquad (2a)$$

$$ETE = H(A\text{–}O^{\bullet}) + H(e^-) - H(A\text{–}O^-) \qquad (2b)$$

SET-PT is another mechanistic pathway that describes heterolytic OH-cleavage (eqn (3)). In the first step of this

mechanism electron leaves molecule forming antioxidant radical-cation specie (A–O$^{\bullet+}$), and in the second step, this radical-cation releases the proton, forming corresponding radical. The first mechanistic step can be estimated based on IP values (Ionization Potential, eqn (3a)), and the second step can be estimated based on PDE values (Proton Dissociation Enthalpy, eqn (3b)). The appropriate enthalpy values for the proton and electron in methanol as a solvent were taken from the literature.[50]

$$A - OH \xrightarrow{-e^-} A - OH^{\bullet+} \xrightarrow{-H^+} A - O^{\bullet} \qquad (3)$$
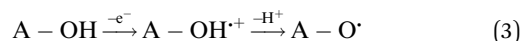
$$IP = H(A\text{–}OH^{\bullet+}) + H(e^-) - H(A\text{–}OH) \qquad (3a)$$

$$PDE = H(A\text{–}O^{\bullet}) + H(H^+) - H(A\text{–}OH^{\bullet+}) \qquad (3b)$$

Conflicts of interest

There are no conflicts to declare.

Acknowledgements

Notes and references

1 B. Halliwell and J. M. M. Gutteridge, *Free Radicals in Biology and Medicine*, 5th edn; Oxford University Press, 2015.
2 I. Liguori, G. Russo, F. Curcio, G. Bulli, L. Aran, D. Della-Morte, G. Gargiulo, G. Testa, F. Cacciatore, D. Bonaduce and P. Abete, *Clin. Interventions Aging*, 2018, **13**, 757–772.
3 C. Sackesen, H. Ercan, E. Dizdar, O. Soyer, P. Gumus, B. N. Tosun, Z. Büyüktuncer, E. Karabulut, T. Besler and O. A. Kalayci, *J. Allergy Clin. Immunol.*, 2008, **122**, 78–85.
4 S. George and H. Abrahamse, *Antioxidants*, 2020, **9**, 1156.
5 A. Taleb, K. Ali Ahmad, A. Ullah Ihsan, J. Qu, N. Lin, K. Hezam, N. Koju, L. Hui and D. Qilong, *Biomed. Pharmacother.*, 2018, **102**, 689–698.
6 M. Sharifi-Rad, N. V. Anil Kumar, P. Zucca, E. M. Varoni, L. Dini, E. Panzarini, J. Rajkovic, P. V. Tsouh Fokou, E. Azzini, I. Peluso, A. Prakash Mishra, M. Nigam, Y. El Rayess, M. E. Beyrouthy, L. Polito, M. Iriti, N. Martins, M. Martorell, O. Docea Anca, W. N. Setzer, D. Calina, W. C. Cho and J. Sharifi-Rad, *Front. Physiol.*, 2020, **11**, DOI: **10.3389/fphys.2020.00694**.
7 M. Bortolami, F. Pandolfi, V. Tudino, A. Messore, V. N. Madia, D. De Vita, R. Di Santo, R. Costi, I. Romeo, S. Alcaro, M. Colone, A. Stringaro, A. Espargaró, R. Sabatè and L. Scipione, *Pharmaceuticals*, 2022, **15**, 673.
8 M. Scipioni, G. Kay, I. Megson and P. K. T. Lin, *Eur. J. Med. Chem.*, 2018, **143**, 745–754.
9 S. B. Nimse and D. Pal, *RSC Adv.*, 2015, **5**, 27986–28006.

10 M. L.-H. Huang, S. Chiang, D. S. Kalinowski, D.-H. Bae, S. Sahni and D. R. Richardson, *Oxid. Med. Cell. Longevity*, 2019, **2019**, 26.

11 V. Thao-Vi Dao, A. I. Casas, G. J. Maghzal, T. Seredenina, N. Kaludercic, N. Robledinos-Anton, F. Di Lisa, R. Stocker, P. Ghezzi, V. Jaquet, A. Cuadrado and H. H. H. W. Schmidt, Pharmacology and Clinical Drug Candidates in Redox Medicine, *Antioxid. Redox Signaling*, 2015, 1113–1129.

12 H. Sies and D. P. Jones, *Nat. Rev. Mol. Cell Biol.*, 2020, **21**, 363–383.

13 H. Sies, C. Berndt and D. P. Jones, *Annu. Rev. Biochem.*, 2017, **20**(86), 715–748.

14 D. P. Jones and H. Sies, The Redox Code, *Antioxid. Redox Signaling*, 2015, 734–746.

15 M. R. Bhosle, L. D. Khillare, I. R. Mali, A. P. Sarkate, D. K. Lokwani and S. V. Tiwari, *New J. Chem.*, 2018, **42**, 18621–18632.

16 F. Buron, J. Y. Mérour, M. Akssira, G. Guillaumet and S. Routier, *Eur. J. Med. Chem.*, 2015, **95**, 76–95.

17 N. Kahriman, K. Peker, V. Serdaroğlu, A. Aydin, A. Usta, S. Fandaklı and N. Yaylıd, *Bioorg. Chem.*, 2020, **99**, 103805.

18 A. R. Saundane, K. Vijaykumar, A. V. Vaijinath and P. Walmik, *Med. Chem. Res.*, 2013, **22**, 806–817.

19 C.-H. Lee, M. Jiang, M. Cowart, G. Gfesser, R. Perner, K. H. Kim, Y. G. Gu, M. Williams, M. F. Jarvis, E. A. Kowaluk, A. O. Stewart and S. S. Bhagwat, *J. Med. Chem.*, 2001, **44**, 2133–2138.

20 M. A. Abdelgawad, M. M. Al-Sanea, A. Musa, M. Elmowafy, A. K. El-Damasy, A. A. Azouz, M. M. Ghoneim and R. B. Bakr, *J. Inflammation Res.*, 2022, **15**, 451–463.

21 Z. Hussain, M. A. Ibrahim, N. M. El-Gohary and A.-S. Badran, *J. Mol. Struct.*, 2022, **1269**, 133870.

22 P. Yadav and K. Shah, *Chem. Biol. Drug Des.*, 2020, **97**, 633–648.

23 S. Wang, X.-H. Yuan, S.-Q. Wang, W. Zhao, X.-B. Chen and B. Yu, *Eur. J. Med. Chem.*, 2021, **214**, 113218.

24 E. Milović, N. Janković, M. Vraneš, S. Stefanović, J. Petronijević, N. Joksimović, J. Muškinja and Z. Ratković, *Environ. Chem. Lett.*, 2021, **19**, 729–736.

25 L. Blaikie, G. Kay and P. K. Thoo Lin, *Bioorg. Med. Chem. Lett.*, 2020, **30**, 127505.

26 W. T. Borden, R. Hoffmann, T. Stuyver and B. Chen, *J. Am. Chem. Soc.*, 2017, **139**, 9010–9018.

27 Ž. Milanović, J. Tošović, S. Marković and Z. Marković, *RSC Adv.*, 2020, **10**, 43262–43272.

28 G. Mazzone, N. Malaj, A. Galano, N. Russo and M. Toscano, *RSC Adv.*, 2015, **5**, 565–575.

29 Z. Marković, M. Filipović, N. Manojlović, A. Amić, S. Jeremić and D. Milenković, *Chem. Pap.*, 2018, **72**, 2785–2793.

30 S. Hwang, Q. Shao, H. Williams, C. Hilty and Y. Q. Gao, *J. Phys. Chem. B*, 2011, **115**, 6653–6660.

31 C. Caratelli, J. Hajek, S. M. J. Rogge, S. Vandenbrande, E. J. Meijer, M. Waroquier and V. Van Speybroeck, *ChemPhysChem*, 2018, **19**, 420–429.

32 S. Jeremić, A. Amić, M. Stanojević-Pirković and Z. Marković, *Org. Biomol. Chem.*, 2018, **16**, 1890–1902.

33 N. H. Attanayake, T. M. Suduwella, Y. Yan, A. P. Kaur, Z. Liang, M. S. Sanford and S. A. Odom, *J. Phys. Chem. C*, 2021, **125**, 14170–14179.

34 N. H. Attanayake, A. P. Kaur, T. M. Suduwella, C. F. Elliott, S. R. Parkin and S. A. Odom, *New J. Chem.*, 2020, **44**, 18138–18148.

35 T. Lunić, J. Lađarević, M. Mandić, V. Veruševski, B. Božić Nedeljković, D. Mijin and B. Božić, *J. Mol. Struct.*, 2022, **1256**, 132546.

36 T. Kundu and A. Pramanik, *Bioorg. Chem.*, 2020, **98**, 103734.

37 Y. Zhao and D. G. Truhlar, *Theor. Chem. Acc.*, 2008, **120**, 215–241.

38 T. H. Dunning Jr, *J. Chem. Phys.*, 1989, **90**, 1007–1023.

39 M. J. Frisch, G. W. Trucks, H. B. Schlegel, G. E. Scuseria, M. A. Robb, J. R. Cheeseman, G. Scalmani, V. Barone, B. Mennucci, G. A. Petersson, H. Nakatsuji, M. Caricato, X. Li, H. P. Hratchian, A. F. Izmaylov, J. Bloino, G. Zheng, J. L. Sonnenberg, M. Hada, M. Ehara, K. Toyota, R. Fukuda, J. Hasegawa, M. Ishida, T. Nakajima, Y. Honda, O. Kitao, H. Nakai, T. Vreven, J. A. Montgomery Jr, J. E. Peralta, F. Ogliaro, M. Bearpark, J. J. Heyd, E. Brothers, K. N. Kudin, V. N. Staroverov, R. Kobayashi, J. Normand, K. Raghavachari, A. Rendell, J. C. Burant, S. S. Iyengar, J. Tomasi, M. Cossi, N. Rega, J. M. Millam, M. Klene, J. E. Knox, J. B. Cross, V. Bakken, C. Adamo, J. Jaramillo, R. Gomperts, R. E. Stratmann, O. Yazyev, A. J. Austin, R. Cammi, C. Pomelli, J. W. Ochterski, R. L. Martin, K. Morokuma, V. G. Zakrzewski, G. A. Voth, P. Salvador, J. J. Dannen-berg, S. Dapprich, A. D. Daniels, Ö. Farkas, J. B. Foresman, J. V. Ortiz, J. Cioslowski and D. J. Fox, *Gaussian 09, Rev D.1 Gaussian Inc*, Wallingford CT, 2013.

40 M. Spiegel, A. Gamian and Z. A. Sroka, *Molecules*, 2021, **26**, 5058.

41 D. S. Dimić, D. A. Milenković, E. H. Avdović, Đ. J. Nakarada, J. M. D. Marković and Z. S. Marković, *Chem. Eng. J.*, 2021, **424**, 130331.

42 D. A. Milenković, D. S. Dimić, E. H. Avdović, A. D. Amić, J. M. D. Marković and Z. S. Marković, *Chem. Eng. J.*, 2020, **395**, 124971.

43 Y. Takano and K. N. Houk, *J. Chem. Theory Comput.*, 2005, **1**, 70–77.

44 E. D. Glendening, J. K. Badenhoop, A. E. Reed, J. E. Carpenter, J. A. Bohmann, C. M. Morales and F. Weinhold, *NBO 5.9*. Theoretical Chemistry Institute, University of Wisconsin, Madison, 2009.

45 J. E. Carpenter and F. Weinhold, *J. Mol. Struct.: THEOCHEM*, 1988, **169**, 41–62.

46 Z. Marković, *J. Serb. Soc. Comput. Mech.*, 2016, **10**, 135–150.

47 E. Klein, V. Lukeš and M. Ilčin, *Chem. Phys.*, 2007, **336**, 51–57.

48 A. Galano, *J. Mex. Chem. Soc.*, 2015, **59**, 231–262.

49 G. Mazzone, A. Galano, J. R. Alvarez-Idaboy and N. Russo, *J. Chem. Inf. Model.*, 2016, **56**, 662–670.

50 Z. Marković, J. Tošović, D. Milenković and S. Marković, *Comput. Theor. Chem.*, 2016, **1077**, 11–17.